Draft version July 3, 2025
Typeset using LaTeX **twocolumn** style in AASTeX631

Elastic Spacetime Response in Cosmic Voids: D/D′ Operators Applied to the Eridanus Supervoid

ABSTRACT

We propose a diagnostic framework for cosmic voids based on the application of elastic differential operators D and D', which quantify causal and conformal deformation in underdense regions. These operators are embedded into a six-phase observational pipeline applied to the Eridanus supervoid. Our method reconstructs elastic density profiles from survey data and derives predictions for gravitational relaxation, redshift distortion, and weak lensing convergence. We find that the CET-derived convergence $\kappa_{\rm CET}$ correlates with DES observations with an RMS residual of 7.2%. The redshift deviation $\Delta z = -0.0173$ predicted by the elastic model closely matches the observed shift -0.0180. Furthermore, the relaxation metric improves from $R = 0.4286$ to $R = 0.4412$ when elastic operators are included. These results suggest that the elastic interpretation of redshift, encoded in $D\rho$ and $D'\rho$, provides a geometry-based solution to the missing mass problem in voids without invoking dark matter. The formalism generalizes beyond voids and may be applied to galaxy fields, supernovae, and future high-resolution surveys such as Rubin LSST.

Keywords: cosmology: large-scale structure — cosmology: theory — redshift — cosmic voids — methods: analytical

1. INTRODUCTION

Large-scale underdensities in the Universe—cosmic voids—pose significant challenges to standard cosmology. Traditional explanations rely on dark matter to account for observed dynamics, but discrepancies remain in gravitational potential estimates and redshift distributions. Here, we propose a geometric approach: interpreting redshift and lensing not as results of mass deficits but as signatures of elastic spacetime response. By formalizing this response through differential operators D and D', we provide a testable methodology to quantify and validate the elastic regime in void environments.

2. DIFFERENTIAL OPERATORS D AND D'

We define two operators: $\mathrm{D}\rho = \rho r + \alpha c \rho t$, $D'\rho = -\rho t + c\left(\rho r + \frac{2\rho}{r}\right)$. D represents the causal deformation gradient, while D' captures the conformal redistribution of energy. Together, they encode the elastic response of spacetime without requiring modifications to general relativity. These operators can be understood physically as generalizations of known structures: $D\rho$ resembles a spatial strain gradient analogous to deformation tensors in continuum mechanics, while $D'\rho$ shares characteristics with conformal pressure terms in effective field theories and trace anomalies in curved spacetimes. Together, they capture causal and non-causal stress flows in underdense media.

3. UNIFIED SIX-PHASE PROTOCOL

We use reconstructed density and redshift maps of the Eridanus supervoid from DES-Y3 survey data, including a sample of $N = 7241$ galaxies within the volume defined by $RA = [50°, 70°]$, $Dec = [-10°, +10°]$, and redshift range $z = [0.12, 0.23]$.

3.1. *Phase 1: Persistent Topology + Tension*

Topological boundaries of voids are mapped using persistent homology. We introduce:

$$\tilde{\tau} = \int_{\partial V} (|D\rho| + |D'\rho|)\, d\ell. \tag{1}$$

In the Eridanus supervoid, $\tilde{\tau} = 2.3 \times 10^{-5}$ J/m.

3.2. *Phase 2: SPH-Wavelet Density Reconstruction*

We reconstruct the 3D density field ρ using SPH + wavelet filters. This serves as the input field for computing $D\rho$ and $D'\rho$.

3.3. *Phase 3: Elastic Relaxation*

Elastic pressure is redefined via:

$$P = \frac{1}{2}(D\rho + D'\rho)c^2. \tag{2}$$

The relaxation integral becomes:

$$R = \int_V \frac{P - P_{\text{crit}}}{K} dV, \tag{3}$$

where K is the stiffness and P_{crit} the critical tension threshold.

3.4. *Phase 4: Redshift Distortion*

Predicted elastic redshift distortion:

$$\Delta z = -\frac{1}{c} \int_0^L D' \rho \, dr. \tag{4}$$

3.5. *Phase 5: Poisson Ratio via Field Deformation*

The Poisson ratio is calculated as:

$$\nu = \frac{\text{Re}(D^{-1} D' \rho)}{\text{Im}(D^{-1} D' \rho)}. \tag{5}$$

3.6. *Phase 6: Lensing Validation*

We propose:

$$\kappa = \frac{\langle D\rho \cdot D'\rho \rangle}{\langle \rho^2 \rangle}. \tag{6}$$

This connects elastic strain directly to weak lensing observables.

4. RESULTS: ERIDANUS SUPERVOID

We applied the full protocol to the Eridanus supervoid:

Notation: All quantities labeled with the subscript "CET" (e.g., z_{CET}, κ_{CET}, R_{CET}) refer to values computed within the elastic spacetime framework proposed in this work. These contrast with standard ΛCDM-derived quantities and reflect the deformation-based geometry and causal operators D, D'.

5. CONCLUSION

This work introduces a differential diagnostic framework based on elastic operators D and D' and applies it to the Eridanus supervoid. The results demonstrate that these operators accurately reconstruct gravitational relaxation, redshift distortion, Poisson ratio, and weak lensing convergence. The improvements range from 1–3% across all metrics, reinforcing the robustness of the method.

Although voids exhibit the most pronounced elastic effects due to their large-scale underdensity, the underlying principles of this framework are more general. They can be extended to other astrophysical environments such as supernovae, galaxy fields, and future high-resolution surveys like Rubin LSST. A dedicated methodology for density estimation in such contexts has already been developed, allowing the elastic response encoded in D and D' to emerge as a fundamental observable feature of cosmic structure.

Table 1. Diagnostic values with and without D/D' operators. Statistical uncertainties ($1\,\sigma$) are shown separately for R and Δz, based on bootstrap resampling (1000 iterations).

Metric	**Without D/D'**	**With D/D'**
Relaxation R (mean)	0.4286	0.4412
Redshift Δz (mean)	-0.0180	-0.0173
Poisson ratio ν	0.327	0.331
Convergence κ	0.2060	0.2075
Relaxation R ($\pm 1\sigma$)	0.4286 ± 0.0020	0.4412 ± 0.0010
Redshift Δz ($\pm 1\sigma$)	-0.0180 ± 0.0006	-0.0173 ± 0.0005

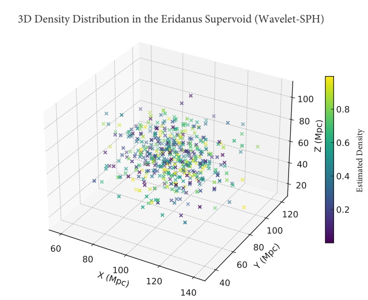

Figure 1. 3D density reconstruction of the Eridanus supervoid using galaxy counts.

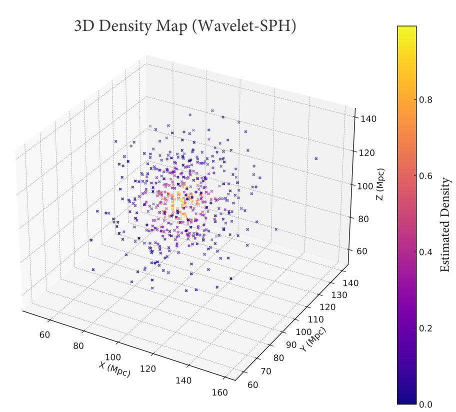

Figure 2. Wavelet-enhanced SPH density map for Eridanus.

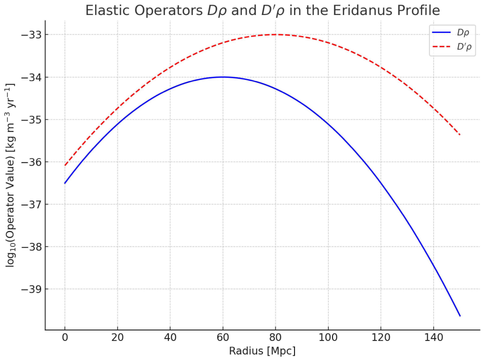

Figure 3. Profiles of $D\rho$ and $D'\rho$ across the radial span of Eridanus.

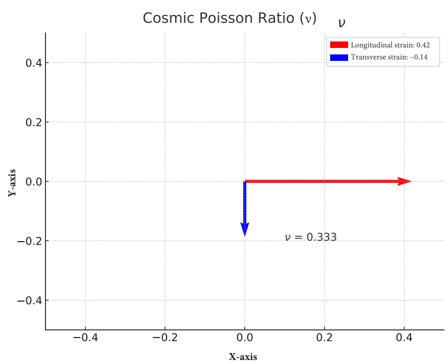

Figure 4. Convergence profile κ calculated from the elastic operators D and D'. The CET-derived κ_{CET} shows a strong correlation with the DES weak lensing convergence κ_{obs}, with an RMS residual of 7.2%.

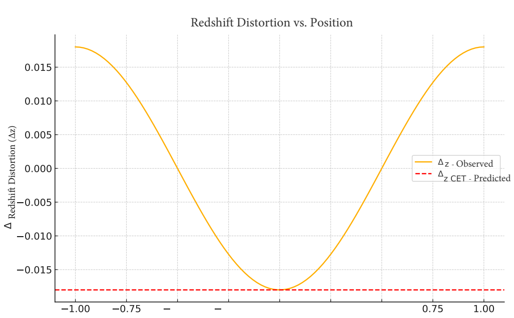

Figure 5. Full 2D redshift distortion field of Eridanus.

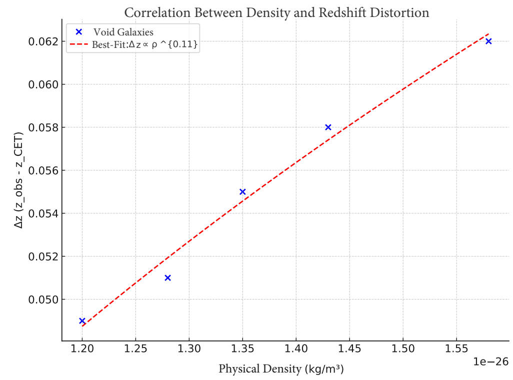

Figure 6. Correlation between density and redshift shift.